



**HAL**  
open science

## Quantifying and simulating carbon and nitrogen mineralization from diverse exogenous organic matters

Florent Levavasseur, Gwenaëlle Lashermes, Bruno Mary, Thierry Morvan, Bernard Nicolardot, Virginie Parnaudeau, Laurent Thuriès, Sabine S. Houot

### ► To cite this version:

Florent Levavasseur, Gwenaëlle Lashermes, Bruno Mary, Thierry Morvan, Bernard Nicolardot, et al.. Quantifying and simulating carbon and nitrogen mineralization from diverse exogenous organic matters. *Soil Use and Management*, 2022, 38 (1), pp.411-425. 10.1111/sum.12745 . hal-03329588

**HAL Id: hal-03329588**

**<https://hal.science/hal-03329588>**

Submitted on 24 Aug 2023

**HAL** is a multi-disciplinary open access archive for the deposit and dissemination of scientific research documents, whether they are published or not. The documents may come from teaching and research institutions in France or abroad, or from public or private research centers.

L'archive ouverte pluridisciplinaire **HAL**, est destinée au dépôt et à la diffusion de documents scientifiques de niveau recherche, publiés ou non, émanant des établissements d'enseignement et de recherche français ou étrangers, des laboratoires publics ou privés.

1 **Quantifying and simulating carbon and nitrogen**  
2 **mineralization from diverse exogenous organic matters**

3 F. LEVAVASSEUR <sup>a,\*</sup>, G. LASHERMES <sup>b</sup>, B. MARY <sup>c</sup>, T. MORVAN <sup>d</sup>, B. NICOLARDOT <sup>e</sup>, V.  
4 PARNAUDEAU <sup>d</sup>, L. THURIÈS <sup>g</sup>, S. HOUOT <sup>a</sup>

5 <sup>a</sup> *INRAE, AgroParisTech, Université Paris-Saclay, UMR ECOSYS, 78850 Thiverval-*  
6 *Grignon, France*

7 <sup>b</sup> *Université de Reims Champagne Ardenne, INRAE, FARE, UMR A 614, 51097 Reims,*  
8 *France*

9 <sup>c</sup> *BioEcoAgro Joint Research Unit, INRAE, Université de Liège, Université de Lille,*  
10 *Université de Picardie Jules Verne, 02000 Barenton-Bugny, France*

11 <sup>d</sup> *UMR SAS, INRAE, Institut Agro, 35000 Rennes, France*

12 <sup>e</sup> *Agroécologie, AgroSup Dijon, INRAE, Univ. Bourgogne, Univ. Bourgogne Franche*  
13 *Comté, 21000 Dijon, France*

14 <sup>g</sup> *CIRAD, UPR Recyclage et Risque, F-97743 Saint-Denis, Réunion, France, Recyclage et*  
15 *Risque, Univ Montpellier, CIRAD, Montpellier*

16 **\*Corresponding Author:** Florent Levavasseur. (E-mail: [florent.levavasseur@inrae.fr](mailto:florent.levavasseur@inrae.fr)).

17 **Running Title:** C and N mineralization from EOM

18

19 **Abstract**

20 The potential contributions of exogenous organic matters (EOMs) to soil organic C and  
21 mineral N supply depend on their C and N mineralization, which can be assessed in  
22 laboratory incubations. Such incubations are essential to calibrate decomposition models,  
23 because not all EOMs can be tested in the field. However, EOM incubations are resource-  
24 intensive. Therefore, easily measurable EOM characteristics that can be useful to predict  
25 EOM behavior are needed.

26 We quantified C and N mineralization during the incubation of 663 EOMs from five  
27 groups (animal manures, composts, sewage sludges, digestates, and others). This  
28 represents one of the largest and diversified set of EOM incubations. The C and N  
29 mineralization varied widely between and within EOM subgroups. We simulated C and N  
30 mineralization with a simple generic decomposition model. Three calibration methods  
31 were compared. Individual EOM calibration of the model yielded good model  
32 performances, while the use of a unique parameter set per EOM subgroup decreased the  
33 model performance, and the use of two EOM characteristics to estimate model parameters  
34 gave an intermediate model performance (average RMSE-C values of 32, 99 and  
35 65 mg C g<sup>-1</sup> added C and average RMSE-N values of 50, 126 and 110 mg N g<sup>-1</sup> added N,  
36 respectively).

37 Because of the EOM variability, individual EOM calibration based on incubation remains  
38 the recommended method for predicting most accurately the C and N mineralization of  
39 EOMs. However, the two alternative calibration methods are sufficient for the simulation  
40 of EOMs without incubation data to obtain reasonable model performances.

41 **Keywords:** organic amendment, fertilizer, model, organic matter, soil, decomposition, N  
42 mineralization

43 **Highlights:**

44 C and N mineralization in 663 exogenous organic matters was quantified under controlled  
45 conditions

46 C and N mineralization varied widely between and among the subgroups of exogenous  
47 organic matters

48 A simple generic model can predict the variability in C and N mineralization from EOMs

49 A calibration was proposed for 26 EOM subgroups using their biochemical characteristics.

50 **1 Introduction**

51 Exogenous organic matter (EOM) is characterized as various residual organic matters  
52 applied to soil as organic fertilizers or organic amendments. They encompass animal  
53 manures and urban and industrial organic wastes and can be used raw or after treatments  
54 (e.g., composting or anaerobic digestion). The contribution of EOM carbon (C) to soil  
55 organic carbon (SOC) and EOM nitrogen (N) to the mineral N supply available to crops  
56 has been extensively studied, especially in long-term field experiments (Gerzabek et al.,  
57 1997; Gómez-Muñoz et al., 2017). A better characterization of the large diversity of EOM  
58 is however needed to better quantify their potential for soil carbon storage, especially  
59 EOMs that have been submitted to treatments such as composting or anaerobic digestion  
60 (Chenu et al., 2019). Due to the limited number of EOMs, cropping systems, and climate  
61 and soil conditions that can be tested *in situ*, many authors have used EOM incubations to  
62 quantify the C and N mineralization of EOMs in soil under controlled conditions (Lazicki  
63 et al., 2020; Mondini et al., 2017; Noirot-Cosson et al., 2017). The kinetics obtained during  
64 laboratory incubations can be used to predict C and N mineralization in field or greenhouse  
65 conditions with additional accounting for the effect of environmental factors (soil  
66 temperature, water content, etc.) (Delin et al., 2012; Gale et al., 2006; Pinto et al., 2020).

67 However, a comparison of the C and N mineralization kinetics of a wide range of common  
68 types of EOM, integrating their variability, is still lacking. EOM incubations can also be  
69 used to calibrate EOM decomposition modules in soil-crop models (Noirot-Cosson et al.,  
70 2016), which allows us to predict the impact of EOM applications under field conditions.  
71 Calibrations for many EOMs have yet to be proposed for the decomposition modules of  
72 soil-crop models, which often do not consider the diversity of and variability in EOMs.  
73 Due to the workload involved in laboratory incubations (several months of incubation are  
74 needed), the use of easily available EOM characteristics (e.g. biochemical fractions and  
75 C:N ratios) to predict C and N mineralization should be encouraged (Delin et al., 2012;  
76 Lashermes et al., 2009, 2010; Lazicki et al., 2020; Morvan & Nicolardot, 2009; Pansu &  
77 Thuriès, 2003; Parnaudeau et al., 2004). The use of these characteristics for calibrating  
78 decomposition modules in soil-crop models should allow prediction not only of the final  
79 mineralization but also the mineralization dynamics; therefore, they need to be validated  
80 for a wide range of EOMs.

81 The aim of this work was to quantify the C and N mineralization of a wide range of EOMs  
82 during laboratory incubations, to test the ability of a simple generic decomposition model  
83 to simulate their C and N mineralization, and to propose some simple calibration methods  
84 of the model in order to avoid the use of long and costly laboratory incubations.

## 85 **2 Materials and methods**

### 86 *2.1 EOM database*

87 The EOM database compiles the results of 663 EOM incubations in soil over at least 90  
88 days under controlled laboratory conditions. The EOM incubations were performed in  
89 various research projects for many years and were not all conducted with exactly the same  
90 procedure. However, most incubations were carried out according to a standard method

91 (AFNOR, 2009): the equivalent of 25 g of dry soil was mixed with the EOM added at a  
92 rate corresponding to 2 g organic C kg<sup>-1</sup> dry soil. The EOM was dried and ground to a  
93 particle size of 1 mm. Mineral N was added in excess to avoid any mineral N deficiency,  
94 which could have limited the EOM decomposition rate, and to highlight the potential N  
95 immobilization (Recous et al., 1995). The temperature was maintained at 28°C, and the  
96 gravimetric water content was equivalent to the field capacity (pF = 2.5). A few  
97 incubations were performed under different conditions (e.g., a temperature of 15°C and a  
98 longer duration and/or with the addition of fresh EOM) (Table S1, Appendix B, online  
99 supporting information). Most soils used in the incubations were loamy and noncalcareous  
100 with a low carbon content (mean soil carbon content equal to 11.6 g kg<sup>-1</sup>, mean soil organic  
101 C:N equal to 9.8) (Table S2, Appendix B, online supporting information).

102 In each incubation, the CO<sub>2</sub> evolved and the soil mineral N were measured to determine  
103 the mineralized C and N. The net C and N mineralized from each EOM were computed by  
104 subtracting the mineralized C and N of an unamended soil (control). The proportions of the  
105 net mineralized C and N from the EOMs were obtained by dividing the net C and N  
106 mineralized from each EOM by the total amount of added organic C and organic N by the  
107 EOM, respectively. We thus hypothesized the absence of a priming effect (Bol et al.,  
108 2003).

109 The EOMs were classified into 5 groups: livestock manures (n=103), composts (n=337),  
110 anaerobic digestates (n=54), sewage sludges (n=70) and others (n=99). Each EOM group  
111 was divided into different EOM subgroups (from 1 to 8). Only digestates were not  
112 subdivided into different subgroups because of the limited number of digestates in the  
113 database compared to the diversity of digestates according to process (solid or liquid state),  
114 post-treatment (phase separation or not), and digested waste (animal manures, urban  
115 wastes) and the non-significant differences in C and N mineralization among these factors.

116 Each EOM was described by its organic C content, its organic and mineral N contents and  
117 its  $C_{org}:N_{org}$  ratio (Table 1). For 608 of the 663 incubated EOMs, the biochemical fractions  
118 of the EOM (Van Soest & Wine, 1967) were also available. These biochemical fractions  
119 combined with the proportion of EOM organic C mineralized during 3 days of incubation  
120 in soil allowed the computation of the  $I_{ROC}$  value, which is an indicator of the proportion of  
121 the EOM organic matter remaining in soils over the long term after application (Lashermes  
122 et al., 2009) (Equation 1).

$$123 \quad I_{ROC} = 44.5 + 0.5 SOL - 0.2 CEL + 0.7 LIC - 2.3 C_{3d} \quad (1)$$

124 where  $SOL$ ,  $CEL$ , and  $LIC$  are the soluble, cellulose-like and lignin-like fractions  
125 (percentage of the total organic matter) and  $C_{3d}$  is the percentage of organic C mineralized  
126 during 3 days of incubation in soil (percentage of the total C)

127 Finally, to estimate the contributions of organic C from the EOMs to the soil organic  
128 matter and of organic N from the EOMs to the soil mineral N, the mineralized organic  
129 carbon and the mineralized organic nitrogen after a period of incubation equivalent to one  
130 year in field conditions based on mean annual temperature were computed. This equivalent  
131 incubation duration was determined by using the concept of “normalized” time (Mary et  
132 al., 1996), which modifies the incubation time with correction factors based on soil  
133 temperature and soil water content. The correction factors of the STICS model were used  
134 (Brisson et al., 2008) (see section 2.2 and Appendix A). The mean annual temperature in  
135 the field applied was 12°C, corresponding to the mean annual temperature in central  
136 France, while a constant soil water content equivalent to field capacity was used. The  
137 observed quantity of C and N mineralized were not modified, only the corresponding  
138 incubation time. For example, 89 days of incubation at 28°C and field capacity  
139 corresponded to 365 days in the field at 12°C and field capacity.

140 2.2 *EOM decomposition model*

141 We used a simple generic decomposition model based on the residue decomposition  
142 module of the STICS model. This model was initially developed for crop residues  
143 (Nicolardot et al., 2001). In this study, we used a modified version of the STICS  
144 decomposition module, adapted from Levavasseur et al. (2021), which allowed a better  
145 simulation of C and N mineralization from EOMs of various origins.

146 The soil organic matter is subdivided into five pools (Figure 1). EOM C is divided into  
147 labile ( $RES_1$ ) and recalcitrant ( $RES_2$ ) pools (with RES standing for “residues”). The  
148 allocation of nitrogen between these two pools can be different, with each pool having its  
149 own C:N ratio ( $CN_{res1}$  and  $CN_{res2}$ ). This allocation is defined by a single parameter,  $a_{CN1}$ ,  
150 which is the ratio between  $CN_{res1}$  and  $CN_{res}$ , where  $CN_{res}$  is the C:N ratio of the EOM as a  
151 whole. The labile pool decomposes according to first-order kinetics with the  
152 decomposition constant  $K_{res}$ , while the recalcitrant pool is directly incorporated into the  
153 active organic matter pool. The decomposed labile pool is either mineralized or assimilated  
154 by the zymogenous microbial biomass pool (with an assimilation yield  $Y$ ). Soil mineral N  
155 may be immobilized if the C:N ratio of the labile pool ( $CN_{res1}$ ) greatly exceeds that of the  
156 microbial biomass ( $CN_{bio}$ ). The microbial biomass decays according to first-order kinetics,  
157 with the decomposition constant  $K_{bio}$ . The decomposed biomass is either mineralized or  
158 incorporated in the active soil organic matter, with the humification yield  $H$ . The soil  
159 mineral N may be immobilized during this decay process depending on the C:N ratio of the  
160 newly formed active soil organic matter, which is set as equal to the initial C:N ratio of the  
161 soil organic matter. The active soil organic matter decomposes according to first-order  
162 kinetics, with the decomposition constant  $K_a$  that depends on soil type (Clivot et al., 2017).  
163 In this study, however, the  $K_a$  constant was optimized to minimize the simulation error of  
164 the mineralized C and N in the control treatment, which did not include EOM in the



165 incubation. The stable soil organic matter pool is assumed to be inert at the century time  
166 scale. With this model, the proportion of mineralized C and N is the sum of three  
167 exponential terms (Appendix A, online supporting information).

### 168 2.3 Model calibration

169 Three methods of calibration (i.e., the adjustment of the model parameters) were tested.  
170 M1 included a calibration specific to each EOM, wherein the unknown decomposition  
171 parameters were optimized for each EOM separately. M2 included a calibration per EOM  
172 subgroup, assuming that all EOMs of the same subgroup had the same optimized  
173 decomposition parameters. M3 included a calibration per EOM subgroup based on  
174 measured EOM characteristics. For the M3 method, the results of the M1 calibration  
175 method were used to derive linear relationships between optimized decomposition  
176 parameters and two EOM characteristics ( $I_{ROC}$  and  $C_{3d}$ ) for all the EOMs together. The  
177 parameters of these linear relationships were further optimized in calibration method M3,  
178 i.e., the decomposition parameters were predicted by using linear relationships with EOM  
179 characteristics. Simple linear functions with only  $I_{ROC}$  and  $C_{3d}$  were selected; other types of  
180 functions and other EOM characteristics available in the database (e.g., lignin content) did  
181 not significantly improve the prediction of the EOM parameters. As for the M2 method,  
182 the interest of the M3 method is to avoid the need for an additional experimental  
183 incubation for each new EOM (i.e., an EOM not in the database). In addition to M2, the  
184 objective of the M3 method is to use easily available EOM characteristics to improve the  
185 calibration within each EOM subgroup.

186 The upper and lower limits of the optimized parameters were mainly determined according  
187 to the literature.  $K_{res}$  varied between 0.005 and 0.7 day<sup>-1</sup>. These values prevented both an  
188 accumulation of the labile pool in soil (which would not be consistent) and unrealistic  
189 decomposition in only a few days.  $K_{bio}$  was set at 0.0076 day<sup>-1</sup> according to Justes et al.

190 (2009), assuming that the zymogenous biomass had the same decay rate for EOMs and  
191 crop residues. The assimilation yield ( $Y$ ) varied between 0.1 and 0.6 (Lee & Schmidt,  
192 2014; Sauvadet et al., 2018; Spohn et al., 2016). The mean value of the humification yield  
193 ( $H$ ) optimized with calibration method M1 was 0.88. Preliminary tests indicated that fixing  
194  $H$  at this value for all EOMs did not significantly decrease model performances (Table S3,  
195 Appendix B, online supporting information) due to compensation between  $H$ ,  $Y$  and  $RES_1$ .  
196 This high and constant  $H$  value is consistent with the primary role of microbial necromass  
197 in soil organic matter formation (Miltner et al., 2012).  $CN_{bio}$  was fixed at 7, according to  
198 the mean value reported in the literature and because the C:N ratio of microbial biomass is  
199 not expected to change markedly (Mooshammer et al., 2014). Fixing  $CN_{bio}$  at this value for  
200 all EOMs did not significantly decrease model performances (Table S3, Appendix B,  
201 online supporting information).  $RES_1$  and  $RES_2$  varied between 0 and 1, allowing EOM to  
202 be completely labile or recalcitrant.  $CN_{res1}$  and  $CN_{res2}$  were defined as positive and to  
203 ensure the nitrogen mass balance (relative to the total amount of N in the EOMs).  
204 For each method of model calibration, the parameters were optimized to minimize the sum  
205 of the root mean square errors ( $RMSEs$ ) for the mineralized C and N (Equation 2).

$$206 \quad RMSE = \sqrt{\frac{1}{n} \cdot \sum_{i=1}^n (O_i - S_i)^2} \quad (2)$$

207 where  $S_i$  and  $O_i$  are the simulated and observed values for the same measurement date ( $i$ )  
208 and  $n$  is the number of measurement dates. The optimized ( $K_{res}$ ) or fixed ( $K_{bio}$ )  
209 decomposition rates were corrected with the temperature and soil water content functions  
210 (Brisson et al., 2008; Mary et al., 1996) (Appendix A) to take into account the effect of  
211 these factors.

212 The “optim” function in R with the “L-BFGS-B” method was used for optimization (Byrd  
213 et al., 1995), giving a lower and an upper bound to each parameter, as mentioned above.

214 2.4 Model validation

215 Calibration method M1 could not be validated on an independent dataset, and the  
216 calibration was specific to each EOM. We assessed the performances of calibration  
217 methods M2 and M3 by using V-fold cross-validation with three replicates. Each EOM  
218 subgroup was randomly divided into three different subsamples. Two subsamples were  
219 used for calibration, and the third subsample was used for validation. We repeated this  
220 operation three times, changing the validation subsample each time, and then repeated  
221 these three operations three times by changing the random division of the sample to avoid  
222 any sampling effects in the results.

223 The performances of the model for calibration and validation were assessed with three  
224 different statistical criteria: the *RMSE*, the mean error (*ME*), and the coefficient of  
225 determination ( $R^2$ ) (Equations 2, 3 and 4). These criteria were computed for each  
226 incubation and then averaged.

227 
$$ME = \frac{1}{n} \cdot \sum_{i=1}^n (O_i - S_i) \quad (3)$$

228 
$$R^2 = \left( \frac{\sum_{i=1}^n ((O_i - \bar{O}) \cdot (S_i - \bar{S}))}{\sqrt{\sum_{i=1}^n (O_i - \bar{O})^2} \cdot \sqrt{\sum_{i=1}^n (S_i - \bar{S})^2}} \right)^2 \quad (4)$$

229 where  $S_i$  and  $O_i$  are the simulated and observed values for the same measurement date ( $i$ )  
230 and  $n$  is the number of measurement dates.  $\bar{O}$  and  $\bar{S}$  are the means of the observations and  
231 simulations, respectively.

232 **3 Results**

233 3.1 Observed C and N mineralization

234 For a given EOM group, the C and N mineralization varied widely between the different  
235 EOMs (Figure 2). For example, for animal manures, the mineralized C varied between 0

236 and 500 mg C g<sup>-1</sup> added C and the mineralized N varied between -500 and 500 mg N g<sup>-1</sup>  
237 added N after twenty days of incubation. Among animal manures, chicken droppings  
238 (AM\_CD) produced the greatest net mineralization, while horse manure decomposition  
239 resulted in a net N immobilization.

240 The calculation of mineralized C after an incubation duration equivalent to one year in the  
241 field allows an easy assessment of the potential EOM contribution to C storage in soil (the  
242 lower the mineralized C is, the higher the contribution) (Figure 3). Compared to all other  
243 EOMs, the lowest values were obtained for composts, with a median C mineralization  
244 equal to 181, 270, 372, 403 and 456 mg C g<sup>-1</sup> added C for composts, digestates, animal  
245 manures, sewage sludges and other EOMs, respectively. However, a large variability was  
246 found within the EOM groups. For example, composts of municipal solid waste (C\_MSW)  
247 exhibited a higher C mineralization (median value of 324 mg C g<sup>-1</sup> added C) than the  
248 average, while composts of green waste (C\_GW) showed a very low C mineralization,  
249 equal to 108 mg C g<sup>-1</sup> added C. Differences in the mineralized C after an incubation  
250 duration equivalent to one year in the field also appeared among animal manures: chicken  
251 droppings, pig slurries and horse manures had median values of 545, 448 and 432 mg C g<sup>-1</sup>  
252 added C, respectively, and were more mineralizable than bovine manure (258 mg C g<sup>-1</sup>  
253 added C). If we consider all the EOM subgroups, the mineralized C after an incubation  
254 duration equivalent to one year in the field appeared to be well correlated with the *I<sub>ROC</sub>* ( $R^2$   
255 = 0.67, Table S4, Appendix B, online supporting information). For specific EOM  
256 subgroups, the *I<sub>ROC</sub>* was also significantly correlated with mineralized C, except for some  
257 EOM subgroups with low mineralization (e.g., green waste compost (C\_GW), Table S4,  
258 Appendix B, online supporting information).

259 The calculation of net mineralized N after an incubation duration equivalent to one year in  
260 the field allowed us to compare the fertilizing values of the various EOMs (Figure 3).

261 Composts and digestates were characterized by a small net mineralization, which varied  
262 between -104 and 76 mg N g<sup>-1</sup> added N. The short-term N fertilizing value of these EOMs  
263 thus relied on their mineral nitrogen content only, which was very low for most composts  
264 (except, e.g., C\_GWS and C\_PIS) but high for digestates (Table 1). Wide variability was  
265 found among the animal manures: horse manure decomposition resulted in strong N  
266 immobilization (-419 mg N g<sup>-1</sup> added N), while chicken droppings produced important net  
267 N mineralization (304 mg N g<sup>-1</sup> added N). Moderate amounts of N were mineralized from  
268 bovine and pig manures (52 and 100 mg N g<sup>-1</sup> added N, respectively), which had small  
269 mineral N contents. The three sewage sludge subgroups exhibited a high mineralized N  
270 (278 to 432 mg N g<sup>-1</sup> added N). The last group of EOMs (“others”) exhibited variable N  
271 mineralization, which is consistent with the highly diverse EOMs within this group,  
272 ranging from vegetal residues (e.g., bark) that mainly immobilized N to algae and animal  
273 residues (e.g., feather meal) that mainly mineralized N. The variability in the net  
274 mineralized N after an incubation duration equivalent to one year in the field for all the  
275 EOM subgroups was partly related to that of *C:N<sub>org</sub>* ( $R^2 = 0.32$ , Table S4, Appendix B,  
276 online supporting information). However, the relationship between the mineralized N and  
277 *C:N<sub>org</sub>* varied widely among the EOM subgroups: a good correlation was observed for  
278 some EOM subgroups (e.g.,  $R^2 = 0.89$  for C\_PIS and  $R^2 = 0.92$  for OTH\_AR) to the  
279 absence of a relationship for other EOMs (e.g.,  $R^2 = 0$  for AM\_HM and SS\_AGR).

### 280 3.2 Prediction of C and N mineralization

281 The simulation of C and N mineralization with a calibration specific to each EOM (M1)  
282 gave very good results. The observed variability was very well accounted for (Figure 4):  
283 the determination coefficient was 0.92 for C and 0.68 for N, the bias was very low  
284 (5 mg C g<sup>-1</sup> added C and 2 mg N g<sup>-1</sup> added N) and the *RMSE* values were 32 mg C g<sup>-1</sup>

285 <sup>1</sup> added C and 50 mg N g<sup>-1</sup> added N (Table 2), which were less than twofold the mean  
286 standard deviation of the observations (17 mg C g<sup>-1</sup> added C and 39 mg N g<sup>-1</sup> added N).

287 When using method M2, which included a calibration per EOM subgroup (i.e., all the  
288 EOMs within the same EOM subgroup had the same optimized parameters), the observed  
289 variability in C and N mineralization was still reproduced by the model (Figure 4), but the  
290 *R*<sup>2</sup> of the cross-validation for N mineralization decreased to 0.52. A slight bias was  
291 observed for C (-11 mg C g<sup>-1</sup> added C), and the *RMSE* increased by a 2- to 3-fold factor for  
292 both C and N (Table 2).

293 When the calibration was based on EOM characteristics (including EOM subgroup) (M3),  
294 the model performance based on the validation dataset was better than the performance  
295 observed for method M2, since the *RMSE* of mineralized C dropped from 99 to 65 mg C g<sup>-1</sup>  
296 <sup>1</sup> added C and the *RMSE* of mineralized N decreased from 126 to 110 mg N g<sup>-1</sup> added N.

297 Regardless of the calibration method, the model performance strongly varied with EOM  
298 subgroup (Tables S3 and S4, Appendix B, online supporting information). For example,  
299 the highest *RMSE* was often associated with the EOM that had the highest mineralization  
300 (e.g. algae (OTH\_ALG) and agri-industrial wastewater (OTH\_AGRWW)).

### 301 3.3 Parameters of the calibration per EOM subgroup

302 For calibration method M2, a set of parameters was proposed for each EOM subgroup  
303 (Table 3). In the absence of a specific incubation for a given EOM or of its characteristics  
304 (e.g., *I<sub>ROC</sub>*), these parameters can be used to simulate C and N mineralization with  
305 acceptable accuracy (section 3.2). The parameters greatly varied according to EOM  
306 subgroup. The labile fraction of the residues (*RES<sub>l</sub>*) varied between 0.13 for the green  
307 waste compost (C\_GW) and 1.00 for vinasse (OTH\_VIN) and algae (OTH\_ALG). The  
308 microbial assimilation yield (*Y*) ranged from 0.10 (for example, in chicken droppings

309 (AM\_CD)) to 0.60 in green waste and sludge compost (C\_GWS). The parameter  $aCN_l$  was  
310 greater than 1 for all EOMs except SS\_AGR, indicating that the C:N ratio of the labile  
311 pool ( $CN_{res1}$ ) was greater than the C:N ratio of the recalcitrant pool ( $CN_{res2}$ ). The  
312 corresponding simulated C and N mineralization dynamics for the different EOM  
313 subgroups are presented in Figure S1 (Appendix C, online supporting information).

#### 314 3.4 Parameters of the calibration per EOM subgroup and with EOM characteristics

315 For calibration method M3, the relationships between the model parameters and EOM  
316 characteristics were established by considering the significant relationships observed  
317 between the optimized parameters of EOM in the first calibration method (M1) and EOM  
318 characteristics (Figure S2). The labile fractions of the EOMs ( $RES_l$ ) decreased with  
319 increasing values of  $I_{ROC}$  ( $R^2=0.61$  with EOM subgroup as a covariable,  $R^2 = 0.49$  for all  
320 the EOMs together). The decomposition rate ( $K_{res}$ ) increased with  $C_{3d}$  according to a  
321 logarithmic relationship ( $R^2 = 0.34$  with EOM subgroup as a covariable,  $R^2 = 0.21$  for all  
322 the EOMs together). The other significant relationships were not considered because they  
323 did not improve the residual variance. The aforementioned linear relationships were  
324 introduced in calibration method M3 to predict the EOM parameters of the model (Table 4  
325 and Table S7, Appendix B, online supporting information). EOM subgroup was added as a  
326 covariable due to the systematic improvement in  $R^2$  when using it.

## 327 4 Discussion

### 328 4.1 Variability in EOM C and N mineralization

329 The comparison of a wide range of EOMs highlighted some important differences in C and  
330 N mineralization among the EOMs (Figure 2, Figure 3). While C mineralization from the  
331 EOMs was generally low for composts, C mineralization can be high for certain EOMs,  
332 such as chicken droppings, animal residues or vinasses. The rate of N mineralization from

333 the EOMs exhibited even more variability between EOM subgroups (e.g., important net N  
334 mineralization for chicken droppings and strong net N immobilization for horse manure).  
335 Considering the organic N content of these two EOMs (Table 1), their typical water  
336 content (60% and 30%, respectively, personal data) and their typical application rate (20  
337 and 3 t ha<sup>-1</sup>, respectively, personal data), the input of organic N would represent  
338 approximately 100 kg ha<sup>-1</sup> in both cases, thus leading to a net immobilization of  
339 42 kg N ha<sup>-1</sup> for horse manure and a net mineralization of 30 kg N ha<sup>-1</sup> for chicken  
340 droppings after one year in the field. Despite the high immobilization caused by horse  
341 manure in the first phase, this EOM could have a fertilizing value during the second phase,  
342 in which N is slowly released (Figure 2). Moreover, it is important to highlight that these  
343 high values of N immobilization represents only the potential immobilization, which can  
344 be reached only when the soil mineral N content is large enough and is a nonlimiting factor  
345 in decomposition. The hierarchy of amendment and fertilizing values between the EOM  
346 subgroups is in line with existing literature (Lazicki et al., 2020; Mondini et al., 2017;  
347 Noirot-Cosson et al., 2017), even though the comparison of so many EOM subgroups is  
348 rare. The hierarchy of mineralized C and N after an incubation duration equivalent to one  
349 year in the field between the EOM subgroups also reflected their contribution to the SOC  
350 (inverse relationship) observed in the field by various authors (Gerzabek et al., 1997;  
351 Levavasseur et al., 2020) and to N short-term supply (Gutser et al., 2005).

352 In addition to the differences between EOM subgroups, a high variability in C and N  
353 mineralization existed inside each EOM subgroup (Figure 3). This result highlighted the  
354 need for a detailed characterization of EOMs, either through laboratory incubations, or  
355 with indicators that are easier to retrieve, such as the *I<sub>ROC</sub>* indicator based on biochemical  
356 fractionation (Lashermes et al., 2009), to determine the contribution of EOMs to SOC. We  
357 found a strong correlation between the mineralized C after an incubation duration



358 equivalent to one year in the field and  $I_{ROC}$  ( $R^2 = 0.67$ ), which was expected because  $I_{ROC}$   
359 was defined as a predictor of residual C in soils under laboratory incubation. Our study,  
360 however, validates the interest of  $I_{ROC}$  for a wider range of EOMs, including for some  
361 EOM subgroups not used in the  $I_{ROC}$  calibration such as digestates ( $R^2$  between mineralized  
362 C and  $I_{ROC}$  equal to 0.62). The mineralized N after an incubation duration equivalent to one  
363 year in the field was less but significantly correlated with EOM characteristics ( $R^2$  with  
364  $CN_{res}$  equal to 0.32), and the correlation was higher for some EOM subgroups (e.g., animal  
365 residues (OTH\_AR)). This result contradicts a study showing that  $CN_{res}$  was a good  
366 predictor of N mineralization ( $R^2 = 0.94$ ) (Lazicki et al., 2020) but confirms another study  
367 pointing out that  $CN_{res}$  is not sufficient for predicting the N mineralization of EOMs of  
368 various qualities (Bonanomi et al., 2019). The limited capacity of this parameter to predict  
369 N mineralization could be explained by the great diversity of EOMs used in our study. For  
370 example, some anaerobic digestates exhibited low  $CN_{res}$  and induced N immobilization, in  
371 opposition to other EOM with low  $CN_{res}$  like sewage sludge. Moreover, the use of  
372 incubations realized in different experimental conditions in our study (temperature, water  
373 content) and their “standardization” using the concept of normalized time (Mary et al.,  
374 1996) could partly weaken the relationship between EOM characteristics and EOM  
375 mineralization for all the incubation taken together, even if most of the EOM incubation  
376 that we used were realized in similar conditions (Tables S1 and S2).

377 Despite the interest in EOM characteristics, they were not sufficient to predict the  
378 dynamics of C and N mineralization in various soil and climate conditions, which required  
379 the use of a well-calibrated decomposition model.

#### 380 4.2 Model performance

381 The calibration of individual EOMs in the model yielded good model performances for all  
382 the EOM subgroups, with  $RMSE$  values equal to 32 mg C g<sup>-1</sup> added C and 50 mg N g<sup>-1</sup>

383 <sup>1</sup> added N and an  $R^2$  equal to 0.92 and 0.68 for C and N mineralization, respectively. These  
384 performances are similar to those reported for other models for a less diverse groups of  
385 EOMs (Gale et al., 2006; Mohanty et al., 2011; Mondini et al., 2017). It is also comparable  
386 to the performance obtained with the STICS model for crop residues (Justes et al., 2009).  
387 When the same set of parameters was used for all the EOMs of the same EOM subgroup,  
388 the model performances decreased for C and N, due to the diversity of EOMs within each  
389 subgroup. The simulation of C mineralization was improved when the EOM characteristics  
390 ( $I_{ROC}$  and  $C_{3ds}$ ) were accounted for in the model parameterization. However, the EOM  
391 characteristics were not sufficient for the determination of decomposition parameters  
392 capable of simulating the N mineralization kinetics very accurately. Such a result was  
393 found by Noirot-Cosson et al. (2017) and Monhanty et al. (2011).

394 Regarding the model performances within the three calibration methods, we recommend  
395 that a specific EOM laboratory incubation is used to calibrate the model (M1 method) and  
396 to most accurately predict its potential behavior in the field, when the user considers a  
397 specific EOM (Figure 5). However, model users often do not have any information on the  
398 particular EOM, except the quantity applied. In that case, we showed that a calibration  
399 depending only on its subgroup (M2 method) bring some insights that are sufficient to test  
400 some global EOM application scenarios. We do not recommend to use the M2 “default”  
401 method to simulate accurately the effects of a specific EOM in case of repeated application  
402 so as not to accumulate over time the error in the estimates. As an alternative to the latter  
403 case, we highly recommend the addition of EOM easily measurable characteristics to  
404 calibrate the model (M3 method), as tested in Levavasseur et al. (2021) for the simulation  
405 of a long term experiment. The quality of the calibration methods M2 and M3 varied  
406 according to the considered EOM subgroup (Table S5 and S6). We recommend the user to  
407 consider the EOM subgroup to determine whether a specific calibration of the modeled

408 EOM (M1) is required or not and to put it in perspective with the objective and  
409 characteristics of the modeling study (e.g., importance of EOM application in the  
410 scenarios).

411 Other EOM characteristics not considered here might contribute to improving the  
412 prediction of EOM model parameters and, subsequently, the simulation of C and N  
413 mineralization. For example, the C:N ratio of biochemical fractions has been shown to be  
414 useful in predicting N mineralization (Morvan & Nicolardot, 2009; Parnaudeau et al.,  
415 2004) as well as <sup>13</sup>C-CPMAS NMR spectral regions (Bonanomi et al., 2019; Pansu et al.,  
416 2017). However, these characteristics were not available in the EOM database we used and  
417 are not usually available outside research laboratories. The identification of readily  
418 available EOM characteristics that can be used to calibrate decomposition models remains  
419 a challenge.

#### 420 *4.3 Model hypotheses*

421 The modification of the STICS model proposed by Levavasseur et al. (2021) to model  
422 EOM decomposition was used to simulate a wide range of EOM decomposition levels in  
423 our study. This modification includes the addition of a recalcitrant pool of EOM that is  
424 directly incorporated in the soil active OM and is not assimilated by the microbial biomass,  
425 assuming that this recalcitrant pool results from the previous digestion of raw matter by  
426 microbial biomass (in animal guts or during treatments). This pool is considered to have  
427 the same dynamics as the active pool in the STICS model. Several authors have  
428 hypothesized that EOM is composed of at least two dynamic pools (Gijsman et al., 2002;  
429 Mondini et al., 2017) to simulate EOM decomposition; however, this distinction was not  
430 necessary for simulating crop residue decomposition in the STICS model, which  
431 considered a single dynamic pool (Justes et al., 2009). Whereas the decay rate of the  
432 recalcitrant pool of EOM was optimized and inferior to the decay rate of the soil active

433 OM in the study of Levvasseur et al. (2021), this decay rate was set equal to that of the  
434 soil active OM in the present study. This simplification caused some overestimation of C  
435 mineralization for very stable EOMs, such as composts (Figure 4). The plateau of C  
436 mineralization usually observed in laboratory incubations could not be properly simulated  
437 with this model. However, this modification was made to limit the number of parameters in  
438 the STICS model. Moreover, several authors have suggested that SOM stability after EOM  
439 application is not modified (Liu et al., 2018; Luan et al., 2019), even though another study  
440 suggested the opposite (Peltre et al., 2017). Levvasseur et al. (2020) successfully  
441 simulated carbon storage in long-term field experiments with EOM application using the  
442 AMG model without assuming a greater stability of EOM in comparison to that of SOM.  
443 Because the STICS and AMG formalisms for SOC are very similar (i.e., SOC is divided  
444 into an active and a stable pool, and the mineralization function is the same) (Clivot et al.,  
445 2019), the STICS model should also allow the simulation of C and N dynamics of EOMs  
446 without assuming a greater stability of those EOMs, i.e., by allocating EOMs only to soil  
447 active OM (either directly, or after soil microbial biomass assimilation, Figure 1). Directly  
448 allocating the recalcitrant fractions of EOMs to soil active OM could change the soil C:N  
449 ratio after repeated applications of the EOMs. This effect is consistent with the fact that  
450 soil C:N usually increases with SOC content (Mooshammer et al., 2014). Other  
451 simplifications made in our study include the use of a constant humification yield ( $H$ ) of  
452 microbial necromass and a constant C:N ratio of microbial biomass ( $CN_{bio}$ ), in line with  
453 recent knowledge about SOM formation (Miltner et al., 2012; Mooshammer et al., 2014).  
454 However, the  $H$  value retained in our study is higher than the value reported in the study of  
455 Miltner et al. (2012). Concerning the decay rate of the labile pool  $K_{res}$ , the calibration  
456 method M1 gave some optimized values equal to the minimal ( $0.005 \text{ day}^{-1}$ ) or maximal  
457 ( $0.7 \text{ day}^{-1}$ ) value for some EOM (Figure S2). The use of lower minimal and higher

458 maximal values could improve the simulation. However, we decided to keep these limits to  
459 prevent both an accumulation of the labile pool in soil (which would not be consistent) and  
460 unrealistic decomposition in only a few days.

461 The use of EOM incubations to calibrate the decomposition module of the STICS model  
462 and predict EOM decomposition under field conditions requires some correction factors  
463 regarding water content and temperature. The use of EOM incubations run under different  
464 conditions (temperature, soil water content, soil type) could have introduced errors into the  
465 EOM calibration, because of the uncertainty associated with these correction factors.  
466 However, most of the EOM incubations used in this study were realized in similar  
467 conditions (loamy soil, 28°C, water content close to or equal to field capacity, Tables S1  
468 and S2). The effects of soil type, water content, temperature and N mineral availability are  
469 already taken into account in the STICS soil-crop model to calculate EOM mineralization  
470 *in situ* (Brisson et al., 2008). The correction factors should allow the extrapolation of  
471 laboratory incubations to field conditions (Gale et al., 2006). However, laboratory  
472 incubations are usually realized with dried and crushed EOM, which can influence the  
473 mineralization of C and, especially, N (Le Roux et al., 2016). Correction factors that  
474 consider EOM preparation before incubation should also be proposed.

475 Finally, beyond the STICS users, the decomposition module (Appendix A) and the  
476 calibrations proposed in this paper could be used outside the STICS model to predict the C  
477 and N mineralization of a large diversity of EOMs.

## 478 **5 Conclusions**

479 We quantified the C and N mineralization of a wide range of EOMs based on a database of  
480 more than 600 EOM incubations, from five groups (animal manures, composts, sewage  
481 sludges, digestates, and others) and 26 subgroups (e.g., bovine manure, green waste

482 compost). This represents one of the largest and most diversified syntheses of EOM  
483 incubation data. The results indicated a wide diversity in EOM contributions to C storage  
484 in soil and N supply for crops, both between EOM subgroups and within EOMs of the  
485 same subgroup. The EOM incubations were used to calibrate a simple generic  
486 decomposition model included in the STICS soil-crop model to simulate EOM  
487 decomposition. Individual EOM calibration yielded the best model performances for the  
488 simulation of C and N mineralization and is the recommended calibration method of the  
489 STICS model for accurate simulations of scenarios of application of a specific EOM in  
490 field conditions. In the absence of EOM incubation data, we proposed two calibration  
491 methods for the 26 different subgroups of EOMs in the STICS model: using either a  
492 unique calibration per EOM subgroup or EOM characteristics as predictors of model  
493 parameters. Although these two calibration methods decreased model performances, they  
494 allow the prediction with a reasonable performance of the EOM contribution to soil C  
495 storage or to mineral N supply to determine the best practices for their use (amount, period  
496 of application, fertilized crops, etc.). Future research is needed to better predict the EOM  
497 parameters from easily available EOM characteristics and verify the extrapolation of  
498 laboratory incubation to field conditions.

## 499 **6 Acknowledgements**

500 We are grateful to the companies LDAR, Auréa, Rittmo and Frayssinet for providing some  
501 of the EOM incubation data.

502

503 **7 References**

- 504 AFNOR. (2009). Norme XP U 44-163. Amendements organiques et supports de culture—  
505 Caractérisation de la matière organique par la minéralisation potentielle du carbone  
506 et de l'azote.
- 507 Bol, R., Moering, J., Kuzyakov, Y., & Amelung, W. (2003). Quantification of priming and  
508 CO<sub>2</sub> respiration sources following slurry-C incorporation into two grassland soils  
509 with different C content. *Rapid Communications in Mass Spectrometry*, 17(23),  
510 2585–2590. <https://doi.org/10.1002/rcm.1184>
- 511 Bonanomi, G., Sarker, T. C., Zotti, M., Cesarano, G., Allevato, E., & Mazzoleni, S. (2019).  
512 Predicting nitrogen mineralization from organic amendments: Beyond C/N ratio by  
513 <sup>13</sup>C-CPMAS NMR approach. *Plant and Soil*, 441(1), 129–146.  
514 <https://doi.org/10.1007/s11104-019-04099-6>
- 515 Brisson, N., Launay, M., Mary, B., & Beaudoin, N. (2008). Conceptual Basis,  
516 Formalisations and Parameterization of the STICS Crop Model (Editions Quae).
- 517 Byrd, R., Lu, P., Nocedal, J., & Zhu, C. (1995). A Limited Memory Algorithm for Bound  
518 Constrained Optimization. *SIAM Journal on Scientific Computing*, 16(5), 1190–  
519 1208. <https://doi.org/10.1137/0916069>
- 520 Chenu, C., Angers, D. A., Barré, P., Derrien, D., Arrouays, D., & Balesdent, J. (2019).  
521 Increasing organic stocks in agricultural soils: Knowledge gaps and potential  
522 innovations. *Soil and Tillage Research*, 188, 41–52.  
523 <https://doi.org/10.1016/j.still.2018.04.011>
- 524 Clivot, H., Mary, B., Valé, M., Cohan, J.-P., Champolivier, L., Piraux, F., Laurent, F., &  
525 Justes, E. (2017). Quantifying in situ and modeling net nitrogen mineralization  
526 from soil organic matter in arable cropping systems. *Soil Biology and*  
527 *Biochemistry*, 111, 44–59. <https://doi.org/10.1016/j.soilbio.2017.03.010>

- 528 Clivot, H., Mouny, J.-C., Duparque, A., Dinh, J.-L., Denoroy, P., Houot, S., Vertès, F.,  
529 Trochard, R., Bouthier, A., Sagot, S., & Mary, B. (2019). Modeling soil organic  
530 carbon evolution in long-term arable experiments with AMG model. *Environmental*  
531 *Modelling & Software*, 118, 99–113. <https://doi.org/10.1016/j.envsoft.2019.04.004>
- 532 Delin, S., Stenberg, B., Nyberg, A., & Brohede, L. (2012). Potential methods for  
533 estimating nitrogen fertilizer value of organic residues. *Soil Use and Management*,  
534 28(3), 283–291. <https://doi.org/10.1111/j.1475-2743.2012.00417.x>
- 535 Gale, E. S., Sullivan, D. M., Cogger, C. G., Bary, A. I., Hemphill, D. D., & Myhre, E. A.  
536 (2006). Estimating Plant-Available Nitrogen Release from Manures, Composts, and  
537 Specialty Products. *Journal of Environmental Quality*, 35(6), 2321–2332.  
538 <https://doi.org/10.2134/jeq2006.0062>
- 539 Gerzabek, M. h., Pichlmayer, F., Kirchmann, H., & Haberhauer, G. (1997). The response  
540 of soil organic matter to manure amendments in a long-term experiment at Ultuna,  
541 Sweden. *European Journal of Soil Science*, 48(2), 273–282.  
542 <https://doi.org/10.1111/j.1365-2389.1997.tb00547.x>
- 543 Gijsman, A. J., Hoogenboom, G., Parton, W. J., & Kerridge, P. C. (2002). Modifying  
544 DSSAT Crop Models for Low-Input Agricultural Systems Using a Soil Organic  
545 Matter–Residue Module from CENTURY. *Agronomy Journal*, 94(3), 462–474.  
546 <https://doi.org/10.2134/agronj2002.4620>
- 547 Gómez-Muñoz, B., Magid, J., & Jensen, L. S. (2017). Nitrogen turnover, crop use  
548 efficiency and soil fertility in a long-term field experiment amended with different  
549 qualities of urban and agricultural waste. *Agriculture, Ecosystems & Environment*,  
550 240, 300–313. <https://doi.org/10.1016/j.agee.2017.01.030>
- 551 Gutser, R., Ebertseder, Th., Weber, A., Schraml, M., & Schmidhalter, U. (2005). Short-  
552 term and residual availability of nitrogen after long-term application of organic



- 553 fertilizers on arable land. *Journal of Plant Nutrition and Soil Science*, 168(4), 439–  
554 446. <https://doi.org/10.1002/jpln.200520510>
- 555 Justes, E., Mary, B., & Nicolardot, B. (2009). Quantifying and modelling C and N  
556 mineralization kinetics of catch crop residues in soil: Parameterization of the  
557 residue decomposition module of STICS model for mature and non mature  
558 residues. *Plant and Soil*, 325(1–2), 171–185. <https://doi.org/10.1007/s11104-009-9966-4>
- 560 Lashermes, G., Nicolardot, B., Parnaudeau, V., Thuriès, L., Chaussod, R., Guillotin, M. L.,  
561 Linères, M., Mary, B., Metzger, L., Morvan, T., Tricaud, A., Villette, C., & Houot,  
562 S. (2009). Indicator of potential residual carbon in soils after exogenous organic  
563 matter application. *European Journal of Soil Science*, 60(2), 297–310.  
564 <https://doi.org/10.1111/j.1365-2389.2008.01110.x>
- 565 Lashermes, G., Nicolardot, B., Parnaudeau, V., Thuriès, L., Chaussod, R., Guillotin, M. L.,  
566 Linères, M., Mary, B., Metzger, L., Morvan, T., Tricaud, A., Villette, C., & Houot,  
567 S. (2010). Typology of exogenous organic matters based on chemical and  
568 biochemical composition to predict potential nitrogen mineralization. *Bioresource  
569 Technology*, 101(1), 157–164. <https://doi.org/10.1016/j.biortech.2009.08.025>
- 570 Lazicki, P., Geisseler, D., & Lloyd, M. (2020). Nitrogen mineralization from organic  
571 amendments is variable but predictable. *Journal of Environmental Quality*, 49(2),  
572 483–495. <https://doi.org/10.1002/jeq2.20030>
- 573 Le Roux, C., Damay, N., Servain, F., Machet, J. M., Houot, S., & Recous, S. (2016, June  
574 27). Effects of crushing and drying organic products on their nitrogen and carbon  
575 mineralization in soil incubations. 19 th Nitrogen Workshop - Efficient use of  
576 different sources of Nitrogen in agriculture – from theory to practice, Skara,  
577 Sweden.

- 578 Lee, Z. M., & Schmidt, T. M. (2014). Bacterial growth efficiency varies in soils under  
579 different land management practices. *Soil Biology and Biochemistry*, 69, 282–290.  
580 <https://doi.org/10.1016/j.soilbio.2013.11.012>
- 581 Levavasseur, F., Mary, B., Christensen, B. T., Duparque, A., Ferchaud, F., Kätterer, T.,  
582 Lagrange, H., Montenach, D., Resseguier, C., & Houot, S. (2020). The simple  
583 AMG model accurately simulates organic carbon storage in soils after repeated  
584 application of exogenous organic matter. *Nutrient Cycling in Agroecosystems*.  
585 <https://doi.org/10.1007/s10705-020-10065-x>
- 586 Levavasseur, F., Mary, B., & Houot, S. (2021). C and N dynamics with repeated organic  
587 amendments can be simulated with the STICS model. *Nutrient Cycling in*  
588 *Agroecosystems*. <https://doi.org/10.1007/s10705-020-10106-5>
- 589 Liu, H., Zhang, J., Ai, Z., Wu, Y., Xu, H., Li, Q., Xue, S., & Liu, G. (2018). 16-Year  
590 fertilization changes the dynamics of soil oxidizable organic carbon fractions and  
591 the stability of soil organic carbon in soybean-corn agroecosystem. *Agriculture,*  
592 *Ecosystems & Environment*, 265, 320–330.  
593 <https://doi.org/10.1016/j.agee.2018.06.032>
- 594 Luan, H., Gao, W., Huang, S., Tang, J., Li, M., Zhang, H., & Chen, X. (2019). Partial  
595 substitution of chemical fertilizer with organic amendments affects soil organic  
596 carbon composition and stability in a greenhouse vegetable production system. *Soil*  
597 *and Tillage Research*, 191, 185–196. <https://doi.org/10.1016/j.still.2019.04.009>
- 598 Mary, B., Recous, S., Darwis, D., & Robin, D. (1996). Interactions between decomposition  
599 of plant residues and nitrogen cycling in soil. *Plant and Soil*, 181(1), 71–82.  
600 <https://doi.org/10.1007/BF00011294>

- 601 Miltner, A., Bombach, P., Schmidt-Brücken, B., & Kästner, M. (2012). SOM genesis:  
602 Microbial biomass as a significant source. *Biogeochemistry*, 111(1), 41–55.  
603 <https://doi.org/10.1007/s10533-011-9658-z>
- 604 Mohanty, M., Reddy, K. S., Probert, M. E., Dalal, R. C., Rao, A. S., & Menzies, N. W.  
605 (2011). Modelling N mineralization from green manure and farmyard manure from  
606 a laboratory incubation study. *Ecological Modelling*, 222(3), 719–726.  
607 <https://doi.org/10.1016/j.ecolmodel.2010.10.027>
- 608 Mondini, C., Cayuela, M. L., Sinicco, T., Fornasier, F., Galvez, A., & Sánchez-Monedero,  
609 M. A. (2017). Modification of the RothC model to simulate soil C mineralization of  
610 exogenous organic matter. *Biogeosciences*, 14(13), 3253–3274.  
611 <https://doi.org/10.5194/bg-14-3253-2017>
- 612 Mooshammer, M., Wanek, W., Zechmeister-Boltenstern, S., & Richter, A. A. (2014).  
613 Stoichiometric imbalances between terrestrial decomposer communities and their  
614 resources: Mechanisms and implications of microbial adaptations to their resources.  
615 *Frontiers in Microbiology*, 5. <https://doi.org/10.3389/fmicb.2014.00022>
- 616 Morvan, T., & Nicolardot, B. (2009). Role of organic fractions on C decomposition and N  
617 mineralization of animal wastes in soil. *Biology and Fertility of Soils*, 45(5), 477–  
618 486. <https://doi.org/10.1007/s00374-009-0355-1>
- 619 Nicolardot, B., Recous, S., & Mary, B. (2001). Simulation of C and N mineralisation  
620 during crop residue decomposition: A simple dynamic model based on the C:N  
621 ratio of the residues. *Plant and Soil*, 228(1), 83–103.  
622 <https://doi.org/10.1023/A:1004813801728>
- 623 Noirot-Cosson, P. E., Dhaouadi, K., Etievant, V., Vaudour, E., & Houot, S. (2017).  
624 Parameterisation of the NCSOIL model to simulate C and N short-term

- 625 mineralisation of exogenous organic matter in different soils. *Soil Biology and*  
626 *Biochemistry*, 104, 128–140. <https://doi.org/10.1016/j.soilbio.2016.10.015>
- 627 Noirot-Cosson, P. E., Vaudour, E., Gilliot, J. M., Gabrielle, B., & Houot, S. (2016).  
628 Modelling the long-term effect of urban waste compost applications on carbon and  
629 nitrogen dynamics in temperate cropland. *Soil Biology and Biochemistry*, 94, 138–  
630 153. <https://doi.org/10.1016/j.soilbio.2015.11.014>
- 631 Pansu, M., & Thuriès, L. (2003). Kinetics of C and N mineralization, N immobilization  
632 and N volatilization of organic inputs in soil. *Soil Biology and Biochemistry*, 35(1),  
633 37–48. [https://doi.org/10.1016/S0038-0717\(02\)00234-1](https://doi.org/10.1016/S0038-0717(02)00234-1)
- 634 Pansu, M., Thuriès, L. J.-M., Soares, V. F., Simões, M. L., & Neto, L. M. (2017).  
635 Modelling the transformation of organic materials in soil with nuclear magnetic  
636 resonance spectra. *European Journal of Soil Science*, 68(1), 90–104.  
637 <https://doi.org/10.1111/ejss.12405>
- 638 Parnaudeau, V., Nicolardot, B., & Pagès, J. (2004). Relevance of Organic Matter Fractions  
639 as Predictors of Wastewater Sludge Mineralization in Soil. *Journal of*  
640 *Environmental Quality*, 33(5), 1885–1894. <https://doi.org/10.2134/jeq2004.1885>
- 641 Peltre, C., Gregorich, E. G., Bruun, S., Jensen, L. S., & Magid, J. (2017). Repeated  
642 application of organic waste affects soil organic matter composition: Evidence from  
643 thermal analysis, FTIR-PAS, amino sugars and lignin biomarkers. *Soil Biology and*  
644 *Biochemistry*, 104, 117–127. <https://doi.org/10.1016/j.soilbio.2016.10.016>
- 645 Pinto, R., Brito, L. M., & Coutinho, J. (2020). Nitrogen Mineralization from Organic  
646 Amendments Predicted by Laboratory and Field Incubations. *Communications in*  
647 *Soil Science and Plant Analysis*, 51(4), 515–526.  
648 <https://doi.org/10.1080/00103624.2020.1717510>

- 649 Recous, S., Robin, D., Darwis, D., & Mary, B. (1995). Soil inorganic N availability: Effect  
650 on maize residue decomposition. *Soil Biology and Biochemistry*, 27(12), 1529–  
651 1538. [https://doi.org/10.1016/0038-0717\(95\)00096-W](https://doi.org/10.1016/0038-0717(95)00096-W)
- 652 Sauvadet, M., Lashermes, G., Alavoine, G., Recous, S., Chauvat, M., Maron, P.-A., &  
653 Bertrand, I. (2018). High carbon use efficiency and low priming effect promote soil  
654 C stabilization under reduced tillage. *Soil Biology and Biochemistry*, 123, 64–73.  
655 <https://doi.org/10.1016/j.soilbio.2018.04.026>
- 656 Spohn, M., Klaus, K., Wanek, W., & Richter, A. (2016). Microbial carbon use efficiency  
657 and biomass turnover times depending on soil depth – Implications for carbon  
658 cycling. *Soil Biology and Biochemistry*, 96, 74–81.  
659 <https://doi.org/10.1016/j.soilbio.2016.01.016>
- 660 Van Soest, P. J., & Wine, R. H. (1967). Use of detergents in the analysis of fibrous feeds.  
661 IV. Determination of plant cell-wall constituents. *Journal of the Association of*  
662 *Official Analytical Chemists*, 50, 50–55.
- 663
- 664

665 **8 Tables**

666

667 **Table 1** Main characteristics of the EOM database

| Group          | Subgroup                                  | Code      | No. of samples | C <sub>org</sub> (g kg <sup>-1</sup> DM) |     | N <sub>org</sub> (g kg <sup>-1</sup> DM) |      | C <sub>org</sub> :N <sub>org</sub> |      | N <sub>min</sub> (g kg <sup>-1</sup> DM) |      | I <sub>ROC</sub> * (%) |    |
|----------------|---|-----------|----------------|--|-----|--|------|------------------------------------|------|--|------|------------------------|----|
|                |   |           |                | Mean                                     | SD  | Mean                                     | SD   | Mean                               | SD   | Mean                                     | SD   | Mean                   | SD |
| Animal manures | Bovine manure                             | AM_BM     | 45             | 359                                      | 69  | 21.1                                     | 5.2  | 18.1                               | 6.5  | 1.3                                      | 1.4  | 59                     | 13 |
|                | Bovine slurry                             | AM_BS     | 3              | 360                                      | 25  | 33.7                                     | 11.2 | 12.0                               | 5.2  | 25.6                                     | 11.3 | 51                     | 6  |
|                | Chicken droppings                         | AM_CD     | 8              | 398                                      | 147 | 45.2                                     | 17.4 | 9.6                                | 3.8  | 2.9                                      | 2.2  | 27                     | 21 |
|                | Horse manure                              | AM_HM     | 8              | 407                                      | 41  | 12.4                                     | 2.4  | 33.6                               | 5.5  | 0.5                                      | 0.5  | 50                     | 5  |
|                | Other manures                             | AM_OTH    | 8              | 366                                      | 75  | 32.9                                     | 12.8 | 12.9                               | 5.2  | 24.8                                     | 40.0 | 58                     | 8  |
|                | Pig manure                                | AM_PIM    | 6              | 428                                      | 29  | 18.1                                     | 3.9  | 24.9                               | 6.9  | 2.4                                      | 1.8  | 57                     | 12 |
|                | Pig slurry                                | AM_PIS    | 10             | 409                                      | 106 | 37.8                                     | 17.1 | 11.9                               | 3.6  | 30.7                                     | 30.2 | 47                     | 10 |
|                | Poultry manure                            | AM_POM    | 15             | 353                                      | 66  | 26.1                                     | 8.5  | 14.2                               | 3.0  | 4.0                                      | 4.6  | 47                     | 19 |
| Composts       | Composted animal manure                   | C_AM      | 39             | 322                                      | 81  | 22.0                                     | 6.8  | 14.9                               | 5.4  | 1.4                                      | 1.8  | 67                     | 14 |
|                | Biowaste and green waste compost          | C_BIO     | 52             | 212                                      | 61  | 16.3                                     | 4.5  | 13.1                               | 2.4  | 0.4                                      | 0.6  | 75                     | 9  |
|                | Green waste compost                       | C_GW      | 25             | 247                                      | 57  | 15.7                                     | 5.3  | 18.2                               | 11.0 | 0.3                                      | 1.3  | 80                     | 7  |
|                | Green waste and animal manure compost     | C_GW+AM   | 9              | 213                                      | 98  | 17.6                                     | 8.7  | 12.4                               | 2.1  | 2.1                                      | 2.1  | 62                     | 12 |
|                | Green waste and sludge compost            | C_GWS     | 71             | 257                                      | 64  | 20.0                                     | 5.2  | 13.6                               | 4.8  | 2.2                                      | 1.8  | 79                     | 10 |
|                | Municipal solid waste compost             | C_MSW     | 89             | 253                                      | 72  | 13.1                                     | 4.1  | 20.1                               | 5.8  | 0.8                                      | 1.0  | 55                     | 15 |
|                | Other composts                            | C_OTH     | 41             | 299                                      | 112 | 17.5                                     | 8.7  | 23.4                               | 22.6 | 1.0                                      | 1.5  | 69                     | 15 |
|                | Pig slurry compost (various cosubstrates) | C_PIS     | 11             | 338                                      | 66  | 22.0                                     | 10.3 | 18.9                               | 10.0 | 3.9                                      | 4.3  | 64                     | 13 |
| Digestates     | All digestates                            | DIG       | 54             | 346                                      | 90  | 26.6                                     | 15.1 | 15.9                               | 7.1  | 36.4                                     | 66.3 | 66                     | 13 |
| Sewage sludges | Agro-industrial sludges                   | SS_AGR    | 11             | 235                                      | 143 | 28.6                                     | 24.4 | 24.5                               | 33.8 | 3.3                                      | 6.2  | 52                     | 15 |
|                | Other sludges                             | SS_OTH    | 6              | 341                                      | 42  | 41.4                                     | 18.0 | 10.5                               | 7.2  | 2.4                                      | 2.0  | 61                     | 3  |
|                | Urban sludges                             | SS_URB    | 53             | 294                                      | 86  | 39.4                                     | 17.5 | 8.9                                | 7.1  | 4.4                                      | 6.1  | 49                     | 17 |
| Others         | Agro-industrial wastewater                | OTH_AGRWW | 23             | 312                                      | 158 | 8.7                                      | 0.7  | 23.4                               | 19.1 | 10.0                                     | 8.3  | -                      | -  |
|                | Algae                                     | OTH_ALG   | 5              | 155                                      | 51  | 13.0                                     | 4.3  | 12.4                               | 1.9  | 0.1                                      | 0.0  | 21                     | 22 |
|                | Animal residues (feather meal, etc.)      | OTH_AR    | 6              | 476                                      | 61  | 103.4                                    | 59.5 | 7.7                                | 6.7  | 5.9                                      | 7.0  | 51                     | 23 |
|                | Others                                    | OTH_OTH   | 38             | 293                                      | 132 | 37.0                                     | 37.2 | 13.8                               | 10.9 | 3.6                                      | 8.5  | 46                     | 23 |
|                | Sugarbeet vinasse                         | OTH_VIN   | 8              | 352                                      | 26  | 34.0                                     | 7.9  | 11.9                               | 2.9  | 1.2                                      | 0.7  | -                      | -  |
|                | Vegetal residues (bark, grape marc, etc.) | OTH_VR    | 19             | 483                                      | 47  | 22.7                                     | 17.7 | 38.5                               | 31.4 | 0.5                                      | 1.4  | 63                     | 16 |

668 \* Indicator of residual organic carbon in soils (Lashermes et al., 2009)

669 **Table 2** Model performance per incubation for all the EOMs together according to the  
670 calibration method (mean calibration and validation performance of the cross-validation  
671 iterations for methods M2 and M3) (ME: mean error, RMSE: root mean square error, R<sup>2</sup>:  
672 coefficient of determination).

| Calibration method                       | Evaluation dataset | Carbon mineralization (mg C g <sup>-1</sup> added C) |      |                | Nitrogen mineralization (mg N g <sup>-1</sup> added N) |      |                |
|--|--------------------|--|------|----------------|--|------|----------------|
|  |                    | ME   | RMSE | R <sup>2</sup> | ME   | RMSE | R <sup>2</sup> |
| M1: Individual EOM calibration           | Calibration        | 5  | 32   | 0.92           | 2  | 50   | 0.68           |
| M2: Calibration per EOM subgroup         | Calibration        | -12  | 91   | 0.91           | 6  | 111  | 0.54           |
|  | Validation         | -11  | 99   | 0.91           | 4  | 126  | 0.52           |
| M3: Calibration with EOM characteristics | Calibration        | -7   | 58   | 0.92           | 11   | 96   | 0.54           |
|  | Validation         | -7   | 65   | 0.92           | 11   | 110  | 0.52           |

673

674



675 **Table 3** Optimized parameters for the STICS decomposition module per EOM subgroup  
676 (obtained with the whole EOM dataset used for calibration method M2).  $K_{bio}$ ,  $H$  and  $CN_{bio}$   
677 were fixed at  $0.0076 \text{ day}^{-1}$ , 0.88 and 7.0, respectively. The meaning of the EOM subgroup can  
678 be found in Table 1.

| EOM subgroup | $K_{res} \text{ (day}^{-1}\text{)}$ | $RES_1$ | Y    | $a_{CN1}$ |
|--------------|-------------------------------------|---------|------|-----------|
| AM_BM        | 0.025                               | 0.24    | 0.32 | 3.09      |
| AM_BS        | 0.062                               | 0.42    | 0.39 | 2.14      |
| AM_CD        | 0.077                               | 0.46    | 0.10 | 1.37      |
| AM_HM        | 0.028                               | 0.48    | 0.31 | 10.00     |
| AM_OTH       | 0.005                               | 1.00    | 0.53 | 1.02      |
| AM_PIM       | 0.011                               | 0.25    | 0.35 | 1.14      |
| AM_PIS       | 0.048                               | 0.40    | 0.10 | 5.25      |
| AM_POM       | 0.055                               | 0.46    | 0.34 | 1.99      |
| C_AM         | 0.005                               | 0.33    | 0.44 | 2.07      |
| C_BIO        | 0.005                               | 0.16    | 0.50 | 10.00     |
| C_GW         | 0.005                               | 0.13    | 0.60 | 10.00     |
| C_GW+AM      | 0.026                               | 0.29    | 0.56 | 10.00     |
| C_GWS        | 0.005                               | 0.18    | 0.60 | 5.58      |
| C_MSW        | 0.059                               | 0.44    | 0.50 | 1.65      |
| C_OTH        | 0.005                               | 0.19    | 0.58 | 4.29      |
| C_PIS        | 0.036                               | 0.34    | 0.57 | 1.04      |
| DIG          | 0.024                               | 0.24    | 0.25 | 10.00     |
| SS_AGR       | 0.090                               | 0.29    | 0.20 | 0.76      |
| SS_OTH       | 0.076                               | 0.48    | 0.52 | 1.04      |
| SS_URB       | 0.072                               | 0.53    | 0.40 | 1.21      |
| OTH_AGRWW    | 0.141                               | 0.64    | 0.38 | 1.71      |
| OTH_ALG      | 0.069                               | 1.00    | 0.25 | 2.38      |
| OTH_AR       | 0.068                               | 0.77    | 0.45 | 1.27      |
| OTH_OTH      | 0.069                               | 0.45    | 0.33 | 1.45      |
| OTH_VIN      | 0.114                               | 1.00    | 0.45 | 1.12      |
| OTH_VR       | 0.013                               | 0.35    | 0.39 | 10.00     |

679

680

681 **Table 4** Calibration for the STICS model per EOM subgroup and according to the EOM  
682 characteristics (M3) (the numerical values of  $\alpha_{res1}$ ,  $\beta_{res1}$ ,  $\alpha_{kres}$ ,  $\beta_{kres}$ ,  $Y$ ,  $a_{CN1}$  per EOM subgroup  
683 are given in Table S7)

| Parameter  | Calibration per EOM subgroup                       |
|------------|--|
| $RES_1$    | $\alpha_{res1} + \beta_{res1} \times I_{ROC}$      |
| $RES_2$    | $1 - RES_2$  |
| $K_{res}$  | $\exp(\alpha_{kres} + \beta_{kres} \times C_{3d})$ |
| $K_{bio}$  | 0.0076   |
| $Y$        | $Y$  |
| $H$        | 0.88   |
| $CN_{bio}$ | 7.0  |
| $a_{CN1}$  | $a_{CN1}$  |

684

685

686 **9 Figure legends**

687 **Figure 1** Decomposition model of EOM in the modified version of the STICS model. The C  
688 fluxes are represented as solid black lines, and the N fluxes are represented as dashed gray  
689 lines.

690  $RES_1$  and  $RES_2$  are the proportions of C from the EOMs in the labile pool and recalcitrant  
691 pools, respectively, with  $RES_2 = 1 - RES_1$

692  $CN_{res}$ ,  $CN_{res1}$  and  $CN_{res2}$  are the C:N ratios of the EOM and the labile and recalcitrant pools,  
693 respectively, and  $a_{CN1}$  is the ratio  $CN_{res1} : CN_{res}$

694  $K_{res1}$  is the decomposition rate of the labile pool

695  $Y$  is the C assimilation yield of the labile pool

696  $CN_{bio}$ ,  $CN_a$  and  $CN_s$  are the C:N ratios of the microbial biomass, and active and stable pools,  
697 respectively

698  $K_{bio}$  and  $K_a$  are the decay rates of the zymogenous biomass and the active soil organic matter  
699 pools, respectively

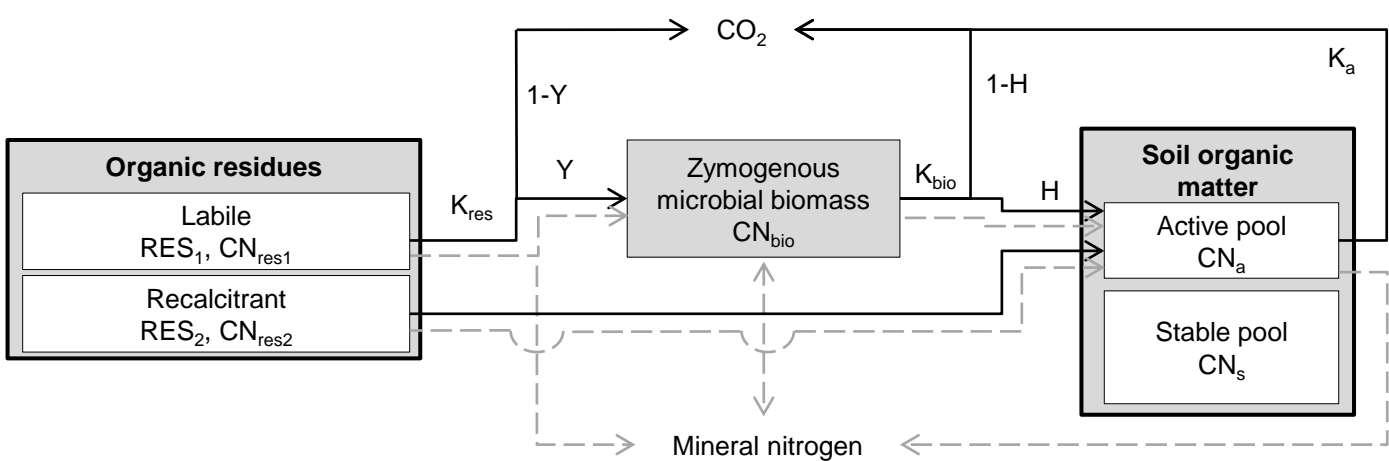
700  $H$  is the C humification yield.

701 **Figure 2** Observed mineralized organic carbon and nitrogen for the different groups of EOMs  
702 in laboratory incubations. Each gray line represents an EOM incubation, while the colored  
703 lines represent fitted local polynomial regressions per EOM subgroup (performed with the  
704 loess function in R). Very few data on N mineralization are lower than -100% and the Y-axis  
705 was cut to -100% to improve the visibility. The meaning of the EOM subgroup abbreviations  
706 can be found in Table 1.

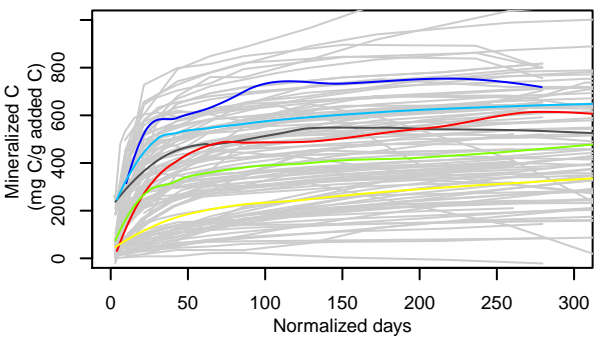
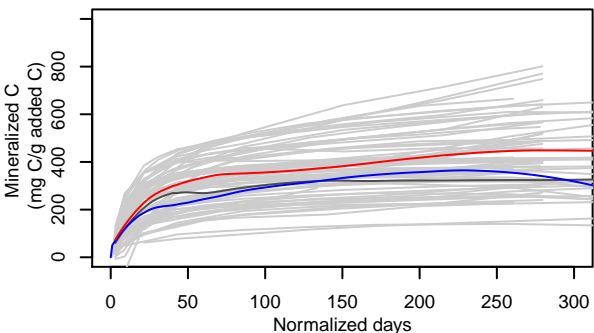
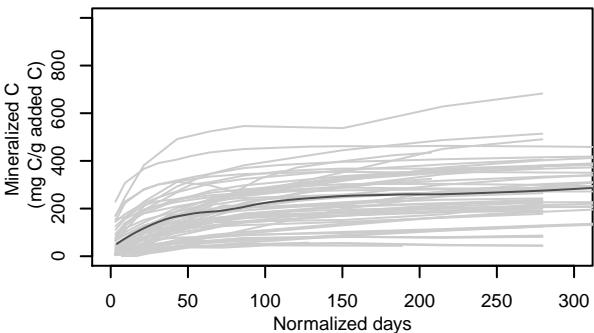
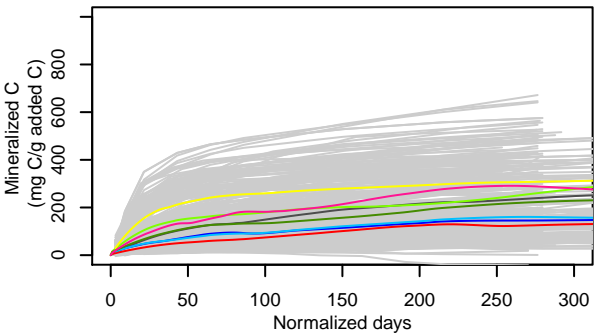
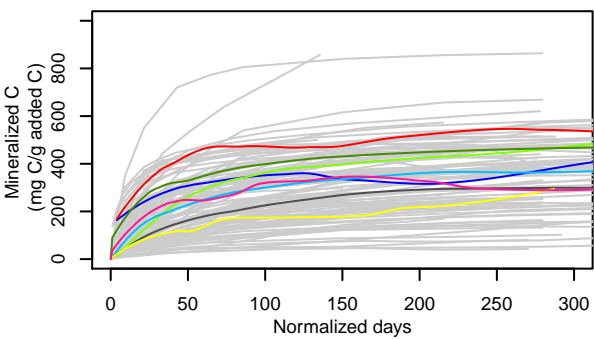
707 **Figure 3** Observed mineralized carbon and net mineralized nitrogen for each EOM group and  
708 subgroup after incubation for a duration equivalent to one year under field conditions. The  
709 meaning of the EOM subgroup abbreviations can be found in Table 1.

710 **Figure 4** Observed and simulated values of carbon and nitrogen mineralization for each EOM  
711 and sampling date, according to the calibration method (results obtained by using the whole  
712 EOM dataset for calibration).

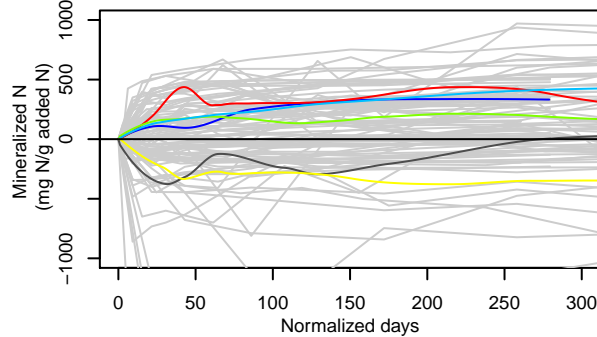
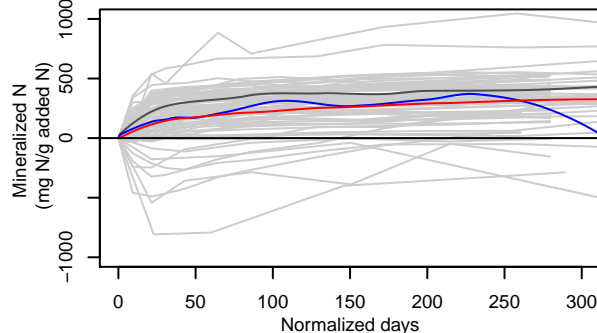
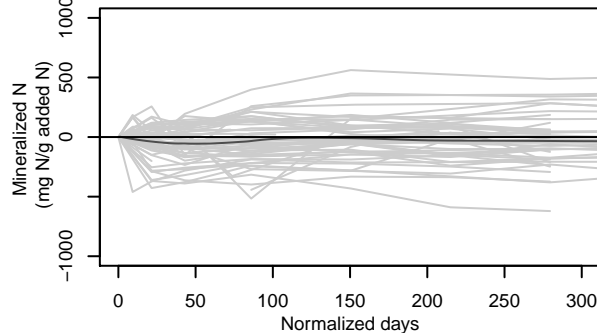
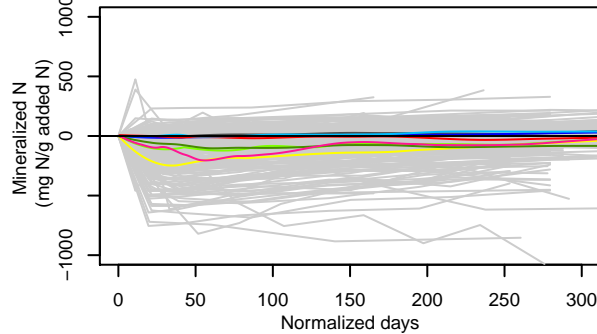
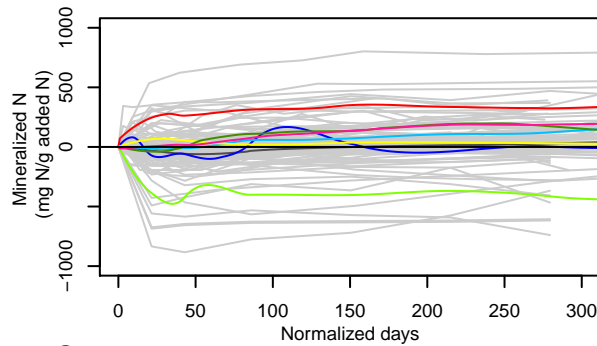
713 **Figure 5.** Conceptual diagram for the calibration of an EOM in the decomposition model.



## Carbon mineralization



## Nitrogen mineralization



### Animal manures

- AM\_BM
- AM\_BS
- AM\_CD
- AM\_HM
- AM\_OTH
- AM\_PIM
- AM\_PIS
- AM\_POM

### Composts

- C\_AM
- C\_BIO
- C\_GW
- C\_GW+AM
- C\_GWS
- C\_MSW
- C\_OTH
- C\_PIS

### Digestates

- DIG

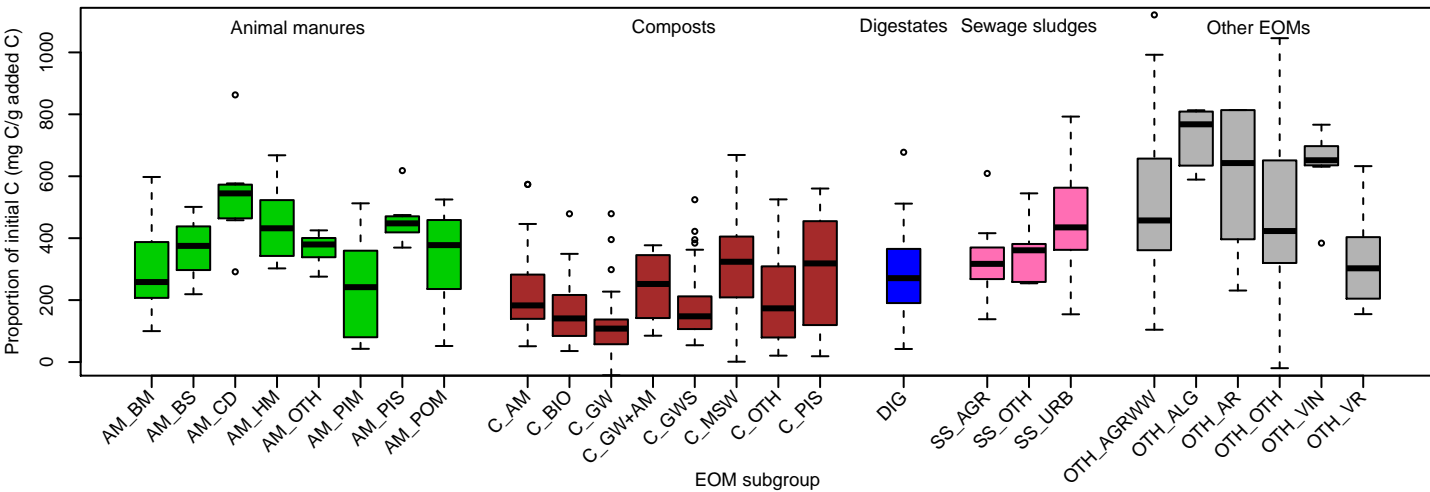
### Sewage sludges

- SS\_AGR
- SS\_OTH
- SS\_URB

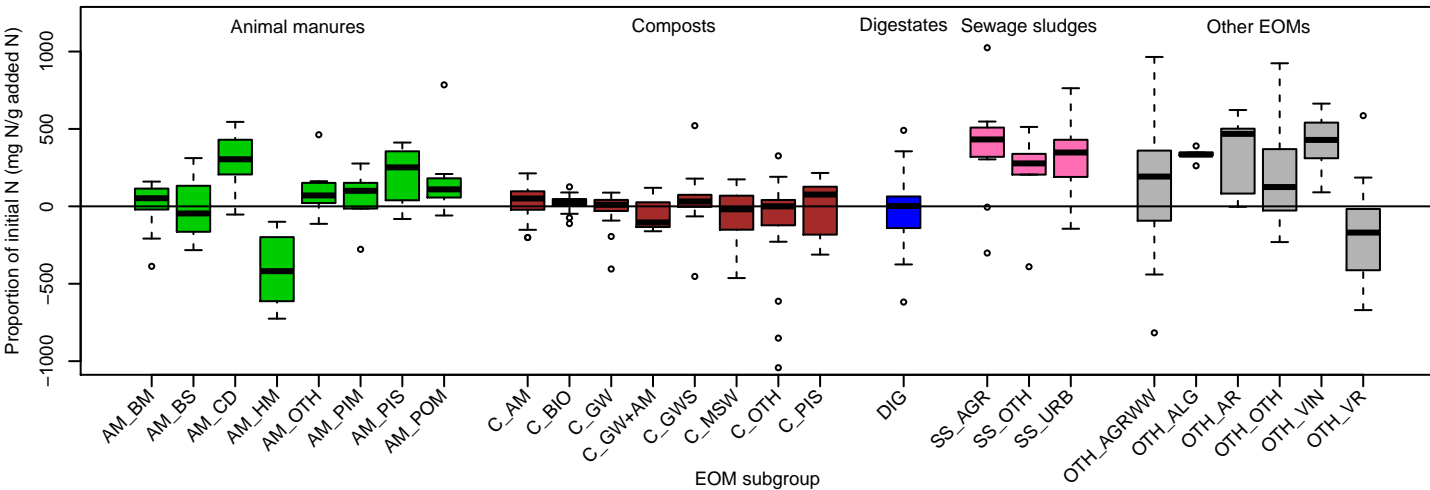
### Other EOMs

- OTH\_AGRWW
- OTH\_ALG
- OTH\_AR
- OTH\_OTH
- OTH\_VIN
- OTH\_VR

## Net mineralized organic C

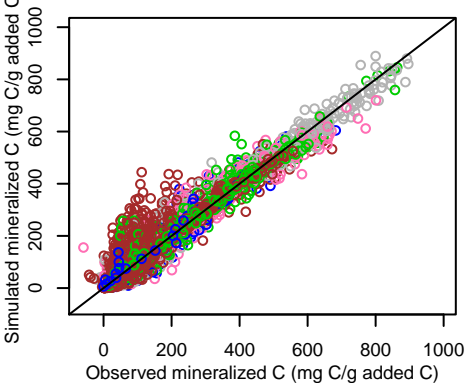


## Net mineralized organic N

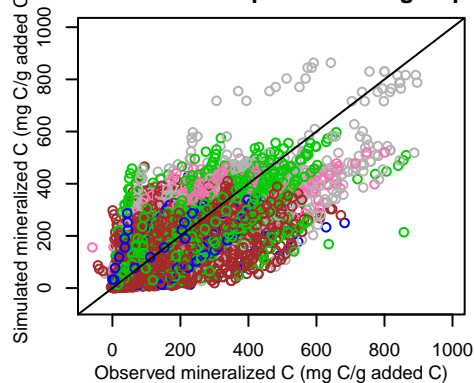


# Carbon mineralization

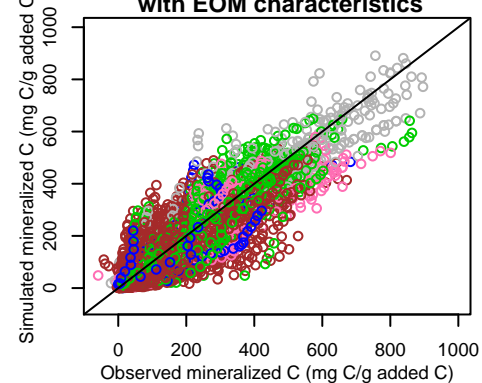
### M1: individual EOM calibration



### M2: calibration per EOM subgroup

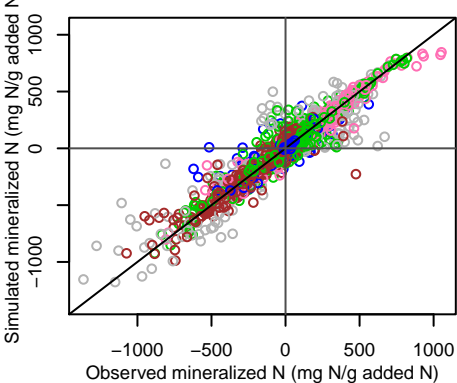


### M3: calibration per EOM subgroup with EOM characteristics

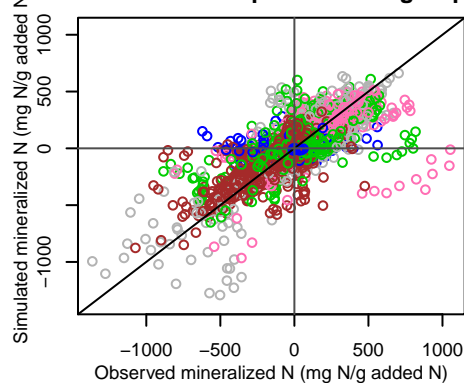


# Nitrogen mineralization

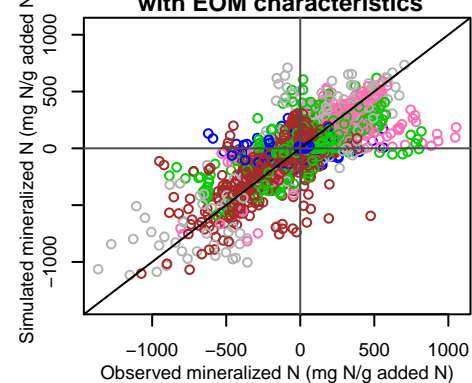
### M1: individual EOM calibration



### M2: calibration per EOM subgroup



### M3: calibration per EOM subgroup with EOM characteristics



● Animal manures ● Composts ● Digestates ● Sewage sludges ● Other EOMs



Experimental data from laboratory incubation for the considered EOM ?

No

Yes

Characteristics ( $I_{ROC}$  and  $C_{3d}$ ) of EOM and subgroup of EOM

Yes

No

**Method 1.** Specific calibration of the model for the considered EOM

- *Best accuracy*
- *Recommended method for an accurate simulation of a specific experiment with repeated EOM application*

**Method 2.** Default model parameter values proposed for the EOM subgroup

- *Lowest accuracy*
- *Sufficient for the simulation of general scenarios of EOM application*

**Method 3.** Model parameters based on the EOM characteristics within each subgroup of EOM

- *Intermediate accuracy*
- *Recommended method for the simulation of a specific experiment in absence of an EOM incubation*